Journal of
Applied
Crystallography
ISSN 0021-8898

Received 25 March 2008
Accepted 13 June 2008



# A novel electrochemical cell for *in situ* neutron diffraction studies of electrode materials for lithium-ion batteries

**Fabio Rosciano, Michael Holzapfel,‡ Werner Scheifele and Petr Novák***

Electrochemistry Laboratory, Paul Scherrer Institut, CH-5232 Villigen PSI, Switzerland. Correspondence e-mail: petr.novak@psi.ch

Lithium-ion batteries are based on the principle of intercalation of lithium ions in host materials, both at the anode and at the cathode. These materials are in general crystalline and, during the operation of the battery, they undergo numerous phase transitions and structural rearrangements, often amplified by the presence of an applied potential difference. While *in situ* X-ray diffraction is an established technique in this field, *in situ* neutron diffraction is still in its pioneering stages and only a few attempts have been made to design an electrochemical cell suitable for these experiments. The technical development of such a device, along with a discussion of its serviceability to combine electrochemical measurements with neutron diffraction experiments, is hereby presented.

## 1. Introduction

Lithium-ion (Li-ion) batteries are the most widely used portable energy source because of their high energy density, their compact design and their long shelf life. Contemporary lithium-ion batteries rely on the insertion of lithium ions into host materials, at both the positive and the negative electrodes. In the positive electrodes, transition metal compounds such as $LiCoO_2$, $LiMn_2O_4$ and $LiFePO_4$ are found (Whittingham, 2004), while the negative electrode market is dominated by carbonaceous materials, particularly graphite (Flandrois & Simon, 1999). All these materials, when subjected to the insertion ('intercalation') and removal ('deintercalation') of lithium ions, undergo structural modifications that range from minor changes in cell parameters to fully fledged phase transitions. The modifications in the crystalline structures of the electrodes are generally metastable and subject to relaxation when the applied potential difference is removed. Furthermore, these intermediate phases, as well as other components such as electrolytes, are often extremely sensitive to oxygen and moisture, therefore compromising the accuracy of *ex situ* and *post mortem* structural investigations. To study in real time the crystallography of the electrode materials it is then necessary to perform reliable *in situ* diffraction experiments that allow a dependable investigation of the changes occurring upon electrochemical charging and discharging.

Numerous *in situ* X-ray diffraction techniques have been suggested in the past, using various approaches to solve the challenge. These range from electrochemical cells that can be used with conventional X-ray diffractometers (Amatucci *et al.*, 1996) to completely automated solutions implemented at synchrotron facilities (Rosciano *et al.*, 2007).

However, *in situ* neutron diffraction has almost been neglected, obviously because of the numerous technical challenges inherent to this particular radiation. The strong incoherent scattering of H atoms present in the electrolyte (usually an organic solution based on carbonates) can be reduced only when expensive deuterated solvents are used. Furthermore, strong neutron absorbers cannot be used as current collectors. Additionally, there is an intrinsic risk of inducing radioactivity in some elements present in the electrode mass, such as cobalt, which becomes heavily activated when irradiated with neutrons.

On the other hand, neutron diffraction offers valuable advantages over X-ray diffraction; the feasibility of detecting light atoms such as lithium is vital in order to estimate directly their positions in the host material's crystal structure, while the ability to distinguish between heavy metals with similar atomic numbers is extremely useful when studying fine differences such as in superstructures. Furthermore, magnetic properties can be investigated.

Considering the field of battery research in a broader sense, an example of an *in situ* cell designed to study aqueous systems by means of neutron diffraction has been presented recently (Bardé *et al.*, 2004), but when limiting the literature search to nonaqueous Li-ion batteries only one attempt has been undertaken to realize an *in situ* electrochemical cell suitable for this technique (Bergström *et al.*, 1998). Hereby we present a completely novel approach to the challenge of *in situ* neutron diffraction, aiming to combine satisfactory electrochemical performance with neutron diffraction measurements.

‡ Present address: Süd Chemie AG, Ostenrieder Strasse 15, D-85368 Moosburg, Germany.

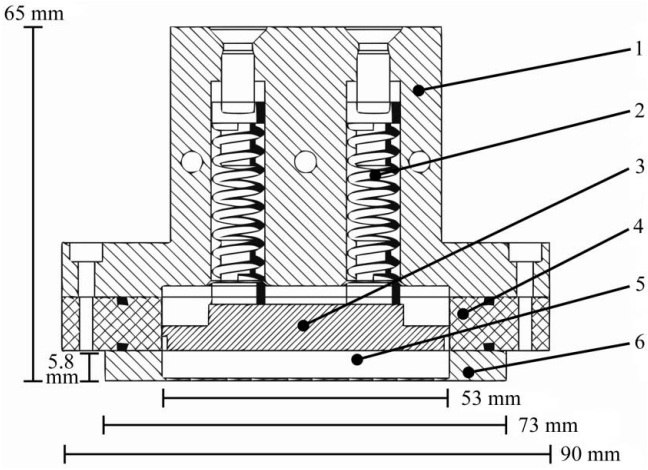


**Figure 1**
Cross section of the assembled device: (1) cell top, (2) spring with piston, (3) negative current collector, (4) cell body, (5) compartment for the active material and entry window for neutrons, (6) positive current collector.

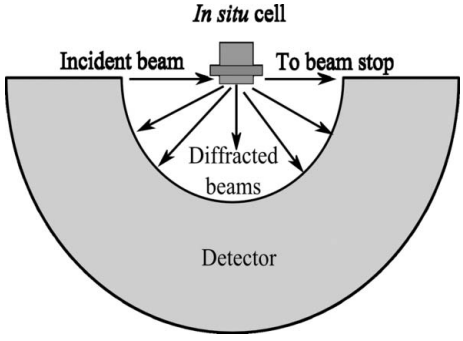


**Figure 2**
Sketch of the beamline setup for the *in situ* measurements. Neutrons enter the sample holder from the side window (53 × 5.8 mm, item 5 in Fig. 1) and the diffracted beams exit through the bottom of the device. Transmitted neutrons exit the cell from the other side to the beam stop. The HRPT diffractometer is in Debye–Scherrer geometry. Drawing not to scale.

## 2. Design of the cell

The electrochemical cell is composed of several construction elements, all visible in Fig. 1. The cell top (1) is made from aluminium and comprises two springs (2) that push on the copper negative current collector (3) in order to maintain the best possible contact between the electrodes. The cell body is made out of polyetheretherketone (PEEK, 4). The cavity into which the electrode material under investigation is pressed (5) is machined into the positive current collector (6), which serves as sample holder. The positive current collector is built from aluminium and has windows for neutrons about 500 μm thick. Aluminium was chosen because of its low neutron absorption coefficient and its reasonably small scattering cross section. The cell body is built out of PEEK because of its very good machinability and inertness to the organic solvents of the electrolyte.

The working electrode is prepared starting from a powder of the particular active material mixed with graphite (to enhance and homogenize the electrical conductivity) and carbon black (an amorphous carbonaceous material that acts as inert filler). The powder blend is thoroughly dry-mixed and then pressed into the cavity of the current collector without adding any polymeric binder. The cavity measures 53 × 5.8 × 19 mm. When measuring diffraction data (see Fig. 2), the incident beam enters the neutron window positioned on the front of the cell (53 × 5.8 mm) and the scattered beam exits from the bottom side of the current collector (53 × 19 mm). The electrode mixture is then dried under vacuum before being transferred to an Ar-filled glove box for cell assembly.

A scheme of the cell assembly is shown in Fig. 3. The electrolyte is added to percolate through the working electrode mass (6), and then a layer of glass fibre separator (5) is placed on the top of it and wetted with electrolyte. A layer of polymeric separator (4) is then put on top to ensure protection against possible formation of dendritic lithium at the counter-electrode. In the next step, the PEEK cell body (item 4 in Fig. 1) is screwed on top of the current collector (7), another glass fibre separator (3) is added and wetted with electrolyte, and finally a strip of metallic lithium (2) is placed on top. The assembly is completed by adding the negative current collector (1) and the cell top (item 1 in Fig. 1), which is firmly screwed to ensure the hermetical tightness of the cell. From that moment the *in situ* cell can be safely handled outside the glove box and is ready to use for experiments.

## 3. Experimental validation of the cell

An *in situ* cell allows use of multiple techniques at the same time, in this case electrochemical characterization and neutron diffraction. Expecting state-of-the-art performance for each particular method is thus unreasonable, but the experimental data from an optimized cell should not be strongly affected by the cell design. To validate the performance of this *in situ* cell, $LiNiO_2$ has been chosen as the model electrode material. Although this compound is not used in commercial batteries owing to its low thermal stability (Dahn *et al.*, 1994) and costly preparation (Morales *et al.*, 1990), it is a good model material because of the extensive literature data on its properties (Ohzuku *et al.*, 1993) and its low activation upon neutron irradiation. Moreover, the structure of $LiNiO_2$ is the same as those of commercially interesting materials such as $LiCoO_2$ and $Li(Mn,Ni,Co)O_2$.

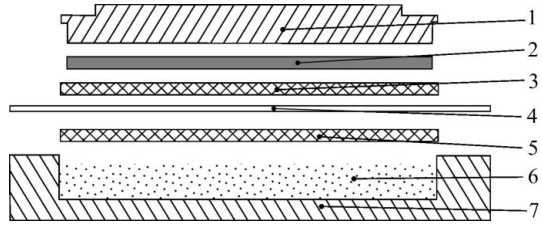


**Figure 3**
Expanded cross section of the electrode assembly: (1) negative current collector, (2) lithium counter-electrode, (3) glass fibre separator, (4) polymeric (Celgard) separator, (5) glass fibre separator, (6) active material, (7) positive current collector and sample holder.

### 3.1. Electrochemical performance

To validate the electrochemical performance of the *in situ* cell, an $LiNiO_2$ electrode has been charged and discharged under similar conditions in a standard laboratory coin-like cell and in our *in situ* cell. The working electrode in the *in situ* cell was a 2:1 wt% mixture of $LiNiO_2$ and carbonaceous materials, while in the coin-like cell the working electrode contained 87% $LiNiO_2$, 8% carbonaceous materials and 5% polymeric binder (polyvinylidene fluoride). The latter is a typical composition for electrochemical experiments. The electric current was adjusted to a *C*/50 rate (*C*/50 means that 50 h are needed to completely charge or discharge the electrode) and the charging was performed from open circuit potential up to 4.5 V *versus* $Li^+/Li$. The counter-electrode was metallic lithium, while the electrolyte was a 1 *M* $LiPF_6$ solution in a 1:1 wt% mixture of ethylene carbonate and dimethylcarbonate. Both cells were in two-electrode configuration, *i.e.* no reference electrode was used. The potential profiles *versus* time are compared in Fig. 4 for the charging period. Owing to the thickness of the working electrode (about 5 mm) there is a certain overpotential in the *in situ* cell that can be quantified as ~120 mV with respect to the coin-like cell. Nonetheless, the potential profiles are very similar for both cells and all expected features ('plateaux' on the charge curve) are clearly identifiable.

### 3.2. Diffraction capabilities

The *in situ* cell was tested at the HRPT diffractometer of the SINQ neutron facility at the Paul Scherrer Institut (Fischer *et al.*, 2000) to assess its suitability for obtaining clear neutron diffraction patterns. $LiNiO_2$ powders were first measured in a standard vanadium tube to refine the cell parameters, which were then compared with those calculated from the patterns of the material contained in a working electrode. The electrode composition was a 2:1 wt% mixture between $LiNiO_2$ and carbonaceous materials. The measurements were conducted with a neutron wavelength of 1.494 Å. In Fig. 5 the pattern obtained with the test $LiNiO_2$ mixture from the *in situ* cell is shown, while the experimental setup is shown in Fig. 2. The neutron powder diffraction pattern was refined using the *FullProf* software package (Rodriguez-Carvajal, 1993) with a three-phase model: $LiNiO_2$, graphite and aluminium. The cell parameters obtained under the standard measuring conditions in the vanadium tube were $a$ = 2.8769 (1) Å and $c$ = 14.189 (9) Å, while those obtained from the *in situ* cell were $a$ = 2.8762 (4) Å and $c$ = 14.185 (3) Å. The model for $LiNiO_2$ included also the refinement of the Li/Ni exchange in the 3*a* site, which amounted to 1% in both experiments, and the refinement of the '$z$' coordinate relative to the O atoms in the 6*c* site, for which the values of 0.241 (7) in the standard sample holder and 0.238 (5) in the *in situ* cell were obtained.

The difference in the values between the measurement performed on $LiNiO_2$ in the standard cylindrical vanadium sample holder and that in the *in situ* cell is comparable to the standard deviation of the parameters, thus confirming the suitability of the *in situ* cell for obtaining meaningful neutron diffraction patterns.

### 3.3. *In situ* measurements on a practical electrode material

The electrochemical *in situ* cell has been used to investigate structural changes of a contemporary positive electrode material for lithium-ion batteries, $Li_{1.1}(Ni_{1/3}Mn_{1/3}Co_{1/3})_{0.9}O_2$. This material shares the same initial crystal structure with $LiNiO_2$ and is classified in the rhombohedral $R\bar{3}m$ space group. The working electrode used for this experiment was a 1:1 wt% mixture between the active material and the carbonaceous materials. The lower active-material-to-carbon

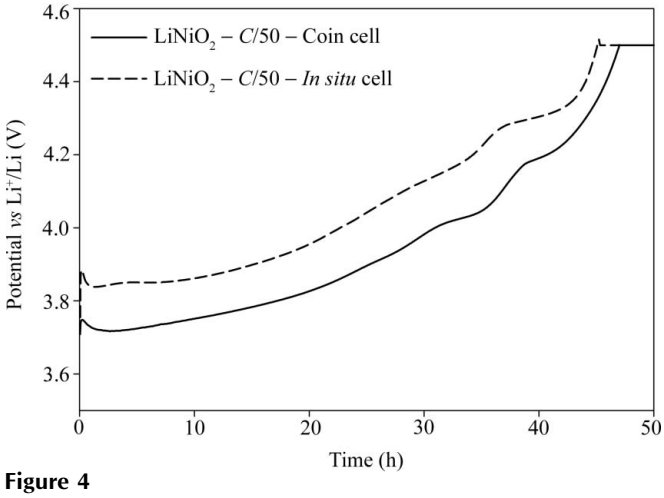


**Figure 4**
Potential profile comparison between the *in situ* cell (dashed line) and a coin-like cell (solid line). The cells were cycled at a *C*/50 rate against an Li counter-electrode in an electrolyte solution of 1 *M* $LiPF_6$ in a 1:1 wt% mixture of ethylene carbonate and dimethyl carbonate in the potential range OCV–4.5 V *versus* $Li^+/Li$.

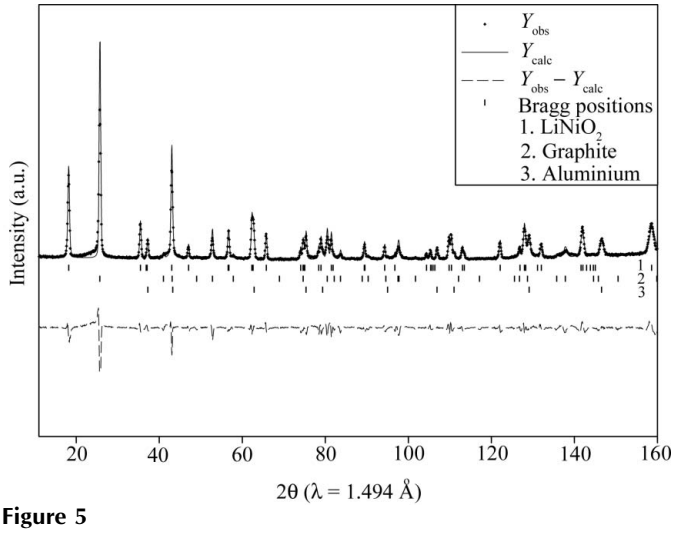


**Figure 5**
Neutron diffraction pattern of a complete electrode measured in the *in situ* cell. The electrode was a dry mixture of $LiNiO_2$, graphite and carbon black enclosed in the aluminium current collector. The electrode was a 2:1 wt% mixture between $LiNiO_2$ and carbonaceous materials and no electrolyte was present. The measurement was performed with a neutron wavelength of 1.494 Å. The plotted Bragg positions are relative to $LiNiO_2$ (top), graphite (middle) and aluminium (bottom).

ratio, when compared with the $LiNiO_2$ test measurement, was needed to improve the electronic conductivity of the electrode mass and thus to decrease the ohmic overpotentials. The full charge of the electrode up to 5.0 V *versus* $Li^+/Li$ was only possible with this setup, as individuated by preliminary laboratory tests. The electrolyte used was a 1 *M* solution of $LiClO_4$ in a 1:1 wt% mixture of ethylene carbonate and dimethyl carbonate (both > 98% deuterated, Armar AG, Döttingen, Switzerland) and the counter-electrode was metallic lithium. Lithium perchlorate was used instead of the standard salt $LiPF_6$ to minimize the risk of side reactions due to water contamination of the deuterated solvents. In Fig. 6 diffraction patterns from the *in situ* cell under electrochemical operation over a full charge with a practical material are shown. It is possible to observe the shift of the [003] peak with the potential. As expected (Kim & Chung, 2004), it is observed that from open circuit potential until 4.5 V *versus* $Li^+/Li$ (corresponding to ∼40% lithium content in the material) the *c* axis of the unit cell increases. Upon further deintercalation of lithium the unit cell shrinks and the [003] peak shifts to higher angles. From Fig. 6 it is clear that the charging of the electrode was homogeneous throughout the entire 5 mm-thick electrode, since only one peak is observed. Thus, this measurement confirmed the suitability of the described *in situ* cell for coupling of electrochemical measurements and neutron diffraction.

### 3.4. Comparison between test measurements and *in situ* measurements

A few words will be spent to comment on the difference in intensity between the [003] peak observed in Fig. 5 and that observed in Fig. 6, as there are many different factors that influence the *in situ* measurements. Firstly, the test measurement on $LiNiO_2$ in Fig. 5 was performed without an electrolyte, whereas the *in situ* measurement in Fig. 6 needed it to allow for the electrochemical charge. As mentioned previously, the electrolyte is a solution of $LiClO_4$ in organic solvents that cause neutron absorption, thus significantly lowering the final intensity of the pattern. Secondly, the background in Fig. 6 is not flat as it is in Fig. 5. This is because during the *in situ* measurement the glass fibre separator (item 5 in Fig. 3) was accidentally in the neutron beam, providing a large bump at low angles and thus 'swallowing' some of the [003] peak shape. Thirdly, $Li_{1.1}(Ni_{1/3}Mn_{1/3}Co_{1/3})_{0.9}O_2$ obviously contained 10% more lithium than $LiNiO_2$ per formula unit, and the absorption due to $^6Li$ was a factor in the overall intensity. Fourthly, the replacement of a strong scatterer such as Ni (coherent scattering length $b$ = 10.3 fm) by less strongly scattering elements such as Mn ($b$ = −3.73 fm) and Co ($b$ = 2.49 fm) (Sears, 1992) decreased the diffracted intensity. If we consider that the intensity is proportional to the square of the structure factor, and that the structure factor is proportional to the scattering length, we obtain that

$$\frac{I_{\mathrm{NiMnCo}}}{I_{\mathrm{Ni}}} = \left[\frac{(1/3)\,(10.3 - 3.73 + 2.49)}{10.3}\right]^2 \simeq 0.086.$$

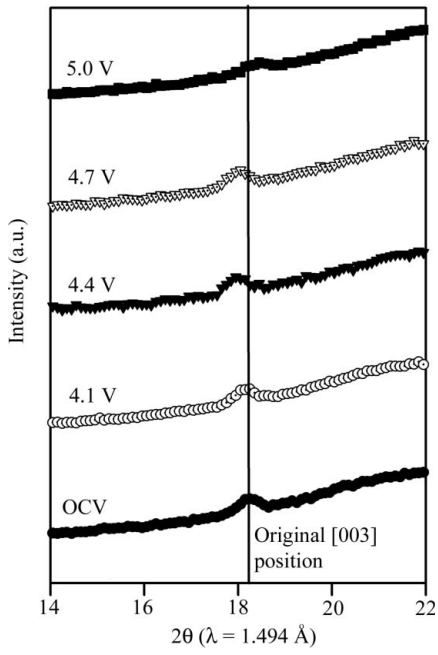


**Figure 6**
Comparison of *in situ* neutron diffraction patterns acquired in full configuration with deuterated electrolyte (1 *M* $LiClO_4$ in a 1:1 wt% mixture of ethylene carbonate and dimethyl carbonate, both > 98% deuterated). The electrode was a 1:1 wt% mixture of $Li_{1.1}(Ni_{1/3}Mn_{1/3}Co_{1/3})_{0.9}O_2$ and carbonaceous materials and was charged against a metallic lithium counter-electrode at the *C* rate of *C*/20. Each measurement was performed with a neutron wavelength of 1.494 Å over a period of 6 h. The [003] peak shift is to lower angles until 4.4 V and to higher angles from 4.7 V. To appreciate the shift, also indicated is the original position of the [003] peak at open circuit voltage (OCV).

Fifthly, as stated above, the need to use a lower active-mass-to-carbon ratio influenced the outcome of the experiment.

These contributions had disrupting effects on the quality of the patterns; however, the experiment demonstrated the viability of the cell concept. We therefore believe that our novel cell is a valuable contribution to the lithium-ion batteries research field and upon careful experiment planning it will be possible to obtain results that will allow for a deeper understanding of the lithium intercalation processes in ceramics for lithium-ion batteries.

## 4. Conclusion

In this work, a novel *in situ* cell suitable for coupling electrochemical measurements with neutron diffraction experiments is presented. The combination of the two techniques led to unavoidable compromises that, however, did not hinder the ability of the cell to deliver meaningful crystal structure data useful, for example, for studying the insertion mechanisms of lithium into electrodes for Li-ion batteries.

The authors would like to acknowledge the technical help of Hermann Kaiser and the kind help of Dr Denis Cheptiakov and Dr Vladimir Pomjakushin at the HRPT beamline.

## References


Amatucci, G. G., Tarascon, J. M. & Klein, L. C. (1996). *J. Electrochem. Soc.* **143**, 1114–1123.

Bardé, F., Palacin, M. R., Chabre, Y., Isnard, O. & Tarascon, J. M. (2004). *Chem. Mater.* **16**, 3936–3948.

Bergstöm, Ö., Andersson, A. M., Edström, K. & Gustafsson, T. (1998). *J. Appl. Cryst.* **31**, 823–825.

Dahn, J. R., Fuller, E. W., Obrovac, M. & Von Sacken, U. (1994). *Solid State Ionics*, **69**, 265–270.

Fischer, P., Frey, G., Koch, M., Könnecke, M., Pomjakushin, V., Schefer, J., Thut, R., Schlumpf, N., Bürge, R., Greuter, U., Bondt, S. & Berruyer, E. (2000). *Physica B*, **276–278**, 146–147.

Flandrois, S. & Simon, B. (1999). *Carbon*, **37**, 165–180.

Kim, J. M. & Chung, H. T. (2004). *Electrochim. Acta*, **49**, 937–944.

Morales, J., Perez-Vincente, C. & Tirado, J. L. (1990). *Mater. Res. Bull.* **25**, 623–630.

Ohzuku, T., Ueda, A. & Nagayama, M. (1993). *J. Electrochem. Soc.* **140**, 1862–1870.

Rodriguez-Carvajal, J. (1993). *Physica B*, **192**, 55–69.

Rosciano, F., Holzapfel, M., Kaiser, H., Scheifele, W., Ruch, P., Hahn, M., Kötz, R. & Novák, P. (2007). *J. Synchrotron Rad.* **14**, 487–491.

Sears, V. F. (1992). *Neutron News*, **3**, 26–37.

Whittingham, M. S. (2004). *Chem. Rev.* **104**, 4271–4301.